A PRELIMINARY APPRAISAL OF ACTIVE FAULT USING GIS AND REMOTE SENSING IN CARBYN CHOWK, PORT BLAIR, SOUTH ANDAMAN, INDIA

A.Sridhar, Ram Raj Mathur, Udaya Laxmi, Jonnalagadda Ravi Department of Geophysics, Osmania University, Hyderabad-500007, Telangana, India sridhargeophysics@gmail.com
S. BalajiG. Department of Disaster Management, Pondicherry University, Port Blair-744112, Andaman and Nicobar Islands, India

ABSTRACT
The surface manifestation geometry of the Carbyn Fault (CF) was inspected using earth observation data (SRTM DEM, Landsat 8 OLI_TIRS & Google Earth Imagery) in Port Blair, South Andaman, India. Primarily, the CF was marked in the study location of Carbyn Chowk, Port Blair with the help of a literature review along with satellite data. The linear structure on the DEM and Landsat 8 images was visually identified. Additionally, the 2D profile of elevation drawn over DEM indicates the presence of a fault line at the intersection of the Ophiolite suite and Andaman flysch. The present study shows the significance and role of satellite remote sensing for active fault studies.

Keywords: Andaman, Active Fault, Carbyn Fault, Remote Sensing, SRTM DEM, Landsat 8.

INTRODUCTION

The union territory of Andaman and Nicobar Islands (ANI) comprises more than six hundred islands, located in the Indian Ocean and has a latitudinal and longitudinal extent of 6° N to 14° N and 92° E to 94° E respectively Figure1(b). After the Great Indian Ocean Earthquake of 9.3 magnitude and Tsunami 2004, these Islands got worldwide attention due to the devastating consequences that resulted in the killing of thousands of people in nearly fourteen countries (Meltzener et al., 2010; Malik et al., 2011). The ANI is a portion of the arc of the Andaman- Nicobar Sumatra Island, located near the trench of Sunda on the Burma Plate (Bhat et al., 2019). In addition, this group of islands is an accretionary wedge that is controlled with sediment and crossed by many active faults (Allen et al., 2007). As a result, these Islands are having a prolonged list of high-magnitude seismic activity, 2009, MW 7.5; 2004, MW 9.3; 2002,
MW 6.8; 1941, MW 7.5; 1881, MW 7.9; 1847, MW 7.5; (Ortiz and Bilham, 2003; Rajendran and Rajendran, 2020; Bilham et al., 2005; Bhat et al., 2022). In the southern part of South Andaman, the Eastern and Central segment mostly occupied by the Carbyn Thrust Fault (CF), has placed the Cretaceous Ophiolites over the Oligocene Andaman Flysch which is nearly in the N-S trending linear zone of deformation (Bhat et al., 2019). The Andaman Flysch, which forms the cover sequences in the western part, subducts along the thrust to a depth of about 17 km (Gokern et al., 2006).
In recent times, the scarp, displaced geomorphic landscapes, topographic ridges, lineaments, and drainage channels have been considered as possible signs of the indicator of active fault movements (Malik et al., 2006; Philip and Virdi, 2006). It is because of the number of evidence for explaining the past fault movement within the landforms being produced by them. Among them, many studies have been completed in the Himalayas (Nakata 1972, 1989; Valdiya 1986, 1993). Earlier, many studies are carried out on active faults in different parts of India using conventional field-based techniques (Nakata 1972, 1989; Valdiya, 1986, 1993). In addition, trench diggings and surface (geomorphology) mapping are also primarily used in conventional paleoseismological active fault studies (McCalpin, 1996, 2009; Machette, M. N., 2000). But recent advancements in science and technologies like remote sensing and geophysical techniques gave an impetus and is perhaps the most inexpensive advanced technique for studying active faults (Philip 1996, Philip and Sah, 1999). Especially, Remote Sensing techniques play a crucial role in understanding the multiple sciences. Many researchers have brought forward the study of the active fault using advanced remote sensing techniques and DEM. (Philip 2007; Armijo et al., 1996; Philip, 1996; San'kov et al., 2000; Karakhanian et al.,

2002; Philip and Virdi, 2006; Ganas et al., 2005; Hooper et al., 2003; Kaya et al., 2004). In recent decades, multi-sensor remote sensing playing a crucial role in identifying and characterizing active faults on a regional scale (Bhat et al., 2019; Gunda et al., 2020). For example, optical remote sensing involves the use of visible and near-infrared light to image the Earth's surface and can be used to identify and map surface features associated with active faults, such as fault scarps and offset drainage patterns (Akinci, A., & Sanli, D. U., 2016). And also, Interferometric Synthetic Aperture Radar (InSAR) has been widely used in mapping active faults, measuring ground deformation, and detecting surface ruptures due to its high- resolution, accurate, and repeatable measurements of surface deformation over time, which helps in identifying the active faults and their associated deformation patterns (Massonnet, D., & Feigl, K. L. 1998). In addition, Light Detection and Ranging (LiDAR) is also an active remote sensing technique that uses laser pulses to measure the distance between the sensor and the target. It also provides highly accurate topographic data, which can be used to identify active faults, map fault scarps, and measure fault displacement (Bilham, R., & Gaur, V. K. 2000). Overall, remote sensing techniques have proven effective for identifying and mapping active faults and can provide valuable information for earthquake hazard assessment and mitigation.

Following the 2004 Great Indian Ocean earthquake, many researchers used various approaches to study the active faults in the Andaman and Nicobar area (ANR). Noteworthy, the well- organized mapping of active faults in quaternary sediments is also striven using the topographic maps and continuous field studies to produce maps of presumed young scarps that result from the tectonic fault region of ANI (Bhat et al., 2019; Gunda et al., 2020). In South Andaman, the Carbyn area is surrounded by significant active faults, but little research has been conducted to identify active faults. Most research focuses on environmental and ecosystem issues, with less emphasis on geological hazards. In ANI, the active fault studies along with a few significant faults disclosed the unbroken signatures of fault movements. With this background, a study of Active Fault Mapping is carried out in Port Blair, the capital of Andaman and Nicobar Islands, using a remote sensing dataset i.e., DEM & Landsat 8 OLI_TIRS.

STUDY AREA AND REGIONAL GEOLOGICAL SETTING

The present study area is located at Carbyn Chowk, Port Blair, South Andaman in 11° 38’14.82’’N latitudes and 92°44’04.97’’ E longitudes (Figure.1). The Carbyn Fault (CF) is a significant and dominant active fault in this region. The CF extends almost 30 kilometers at the Eastern portion of South Andaman and passes through the Kodiyaghat and Burmanallah between Carbyn and Chidiyatapu (Bhat et al., 2019). This CF is an N-S trending linear deformation zone and has deposited Cretaceous ophiolites above Oligocene Andaman Flysch (Naik G. C. et al., 1997). In addition, this CF splits the prominent N-S-trending dissected Ophiolite body which is found at various structural planes from the siliciclastic turbidites (Andaman Flysch) (Bhat et al., 2019) (Figure.2) and is also known that these Ophiolite sequences are made up of tectonic cumulate plagiogranite-diorite and suite-basalt-pelagic sediments that is a preserved section of oceanic crust (Pal, T. et al., 2005). Meta sediment and Meta basalt units connected to ophiolites are important for understanding the history of the thrust's emplacement (Mishra, S. et al., 2019). The Upper Eocene to Oligocene-aged Sandstone, Siltstone, Grit, Conglomerate, Limestone, and Shale are interbedded in the Andaman Flysch formations (Bandopadhyay, P. C. et al., 2012). In an accretionary prism environment, thrust contact with Andaman Flysch demonstrates the thrust-controlled emplacement via off-scraping from the subducting plate or the lower half of the wedge (Moores et al., 1984; Pal, T. et al., 2020). As a result of subduction, the subducting slab's ocean crust (Ophiolite) was scraped off and deposited as a thrust slice (Pal, T. et al., 2020).

REMOTE SENSING DATA PROCESSING

A number of Remote Sensing earth observation data was used in the current study (Table: 1). primarily, the first step consists of a base map preparation of the study area using the Survey of India toposheet (toposheet no. 87A10). For fault mapping of the study location, hill-shaded Shuttle Radar Topography

Mission (SRTM) DEM of 30 spatial resolution was used which was registered with the UTM spatial reference system (WGS 84 Zone 46N) (Figure.3). Digital elevation models (DEM) are useful for identifying structural details on the surface of the earth and for revealing the surface expressions of the geomorphology of the earth (Teichrieb and Kelner). Further, it is confirmed on pan-sharpened Landsat 8 OLI_TIRS processed in Arc GIS using a composite band of 2,3,4,5 and 8 (Figure.4). Moreover, it is marked using Google earth pro image followed by an extensive field survey.

RESULTS AND DISCUSSION

REMOTE SENSING DATA ANALYSIS

The current study utilized the SRTM 30 m DEM to identify and demarcate the significant active thrust fault. The geomorphology of the Carbyn thrust's northern section is very well defined, complicated, and appears to be highly sharp from Carbyn to the Burmanallah region (Figure. 3). Several 2D topographic profiles were generated using the SRTM-DEM and the best profile was utilized to extract the Carbyn active thrust fault (Figure.3a). The primary displacement zone between the Ophiolite Suite and the Andaman Flysch is represented by a long, extended basin that runs perpendicular to the scarp. The Carbyn fault trending N-S to NE-SW was also plotted using Landsat 8 OLI_TIRS (Figure.4) and Google Earth images. Field investigations allowed us to confirm and locate active fault traces in South Andaman, including noticeable fault scarps, pressure ridges, elevated marine terraces, uplifted coral beds, and other structures linked to recent deformations.we also clearly delineated parallel active faults and folds with a wavelength of a few kilometers, which are broadly running from N-S to NE-SW. This allows for the visualization of several N-S trending active thrust fault lines and active emergent folds. The bulk of fold trends appear to be absorbing a sizable percentage of the plate boundary strain and are compatible with the thrust trace, which indicates E-W shortening. This fault has a rectilinear drainage pattern running along it and has impounded straight. Moreover, these springs, depressions in the terrain, and vegetation are all parallel to the fault's strike. Along the fault zone, we also saw several unconfined springs that provide the area with groundwater.

CONCLUSION

Earth observation data SRTM DEM, Landsat 8 OLI_TIRS, & Google Earth Imagery were used to examine the surface manifestation geometry of the Carbyn Fault (CF). Visual identification was possible of the linear structure in the DEM and Landsat 8 Images. Further evidence of a fault line at the junction of the Ophiolite suite and Andaman flysch comes from the 2D profile of elevation produced over DEM. This study demonstrates the value and application of satellite remote sensing for investigations of the Carbyn active fault in the Carbyn area, Port Blair, India.

Acknowledgments

We are thankful to the Department of Geophysics, Osmania University, Hyderabad, India for providing institutional support to carry out this study.

References

1. Allen, R., Carter A., Najman, Y., Bandopadhyay, PC., Chapman, HJ., Bickle, M.J., Garzanti, E., Vezzoli, G., Andò, S., Foster, G.L. and Gerring, C. (2007) New constraints on the sedimentation and uplift history of the Andaman-Nicobar accretionary prism, South Andaman Island. In: Draut, A., Clift, P.D., Scholl, D.W. (Eds.), Formation and applications of the sedimentary record in arc collision zones. Geol. Soc. Amer. Spec. Paper, v.436, pp.223–254.
2. Akinci, A., & Sanli, D. U. (2016). Detection of active faults using satellite imagery and aerial photographs: A case study from Turkey. Journal of Asian Earth Sciences, 120, 60-68.
3. Armijo, R., Meyer, B. and King, G.C.P., 1996, Quaternary evolution of the Corinth Rift and its implications for the late Cenozoic evolution of the Aegean. Geophysical Journal International, 126, pp. 11–53.

4. Bandopadhyay, P. C. (2012). Re-interpretation of the age and environment of deposition of Paleogene turbidites in the Andaman and Nicobar Islands, Western Sunda Arc. Journal of Asian Earth Sciences, 45, 126-137.
5. Bhat, G. R., Balaji, S., & Yousuf, M. (2022). Tectonic geomorphology and seismic hazard of the east boundary thrust in northern segment of the Sunda–Andaman subduction zone. Natural Hazards, 1-23.
6. Bhat, G. R., Balaji, S., Iqbal, V., Balakrishna, B., & Yousuf, M. (2019). Neotectonics and related crustal deformation along Carbyn thrust fault, South Andaman, India: implications of the frontal surface faulting and propagation of tectonic activity towards Andaman trench. Arabian Journal of Geosciences, 12, 1-13.
7. Bilham, R., Engdahl, R., Feldl, N., & Satyabala, S. P. (2005). Partial and complete rupture of the Indo-Andaman plate boundary 1847-2004. Seismological Research Letters, 76(3), 299-311.
8. Bilham, R., & Gaur, V. K. (2000). LiDAR elevation models of the 1999 Chamoli earthquake region and the evolution of surface deformation in the Himalaya Geophysical Research Letters, 27(24), 4077-4080.
9. Ganas, A., Pavildes, S. and Karastathis, V., 2005, DEM-based morphometry of range front escarpments in Attica, Central Greece, and its relation to fault slip rates. Geomorphology, 65, pp. 301–319.
10. Gunda Goutham Krishna Teja, Balaji S., Ray Champati P.K., Bhat Gulam Rasool, Balakrishna and Kannaujiya S. (2020) Geophysical Characterisation of the Active Fault Geometry and Trends in Tectonic Deformation in the Shallow Stratigraphy along Active Faults, South Andaman, India. Journal Geological Society of India Vol.95, March 2020, pp.286-292.
11. Hooper, D.M., Bursik, M.I. and Webb, F.H., 2003, Application of high resolution, interferometric DEMs to geomorphic studies of fault scarps, Fish Lake Valley, Nevada- California, USA. Remote Sensing of Environment, 84, pp. 255–267.
12. Karakhanian, A., Djrbashian, R., Trifonov, V., Philip, H., Arakelian, S. and Avagian, A., 2002, Holocene-historical volcanism and active faults as natural risk factors for Armenia and adjacent countries. Journal of Volcanology and Geothermal Research, 113, pp. 319–344.
13. Kaya, S., Muftuoglu, O. and Tuysuz, O., 2004, Tracing the geometry of an active fault using remote sensing and digital elevation model: Ganos segment, North Anatolian Fault zone, Turkey. International Journal of Remote Sensing, 25, pp. 3843–3855.
14. Khalifa, A.; Cakir, Z.; Owen, L.A. and Kaya, S. (2019) Evaluation of the Relative Tectonic Activity of the Adıyaman fault within the Arabian-Anatolian plate boundary (eastern Turkey). Geologica acta: an international earth science journal, ISSN 1695- 6133, Vol. 17, No. 1, 2019, 17 page.
15. Machette, M. N. (2000). Active, capable, and potentially active faults—a paleoseismic perspective. Journal of Geodynamics, 29(3-5), 387-392.
16. Malik, J. N., Murty, C. V. R., & Rai, D. C. (2006). Landscape changes in the Andaman and Nicobar Islands (India) after the December 2004 great Sumatra earthquake and Indian Ocean tsunami. Earthquake Spectra, 22(3_suppl), 43-66.
17. Malik, J. N., Shishikura, M., Echigo, T., Ikeda, Y., Satake, K., Kayanne, H., & Dikshit, O. (2011). Geologic evidence for two pre-2004 earthquakes during recent centuries near Port Blair, South Andaman Island, India. Geology, 39(6), 559-562.
18. Massonnet, D., & Feigl, K. L. (1998). Radar interferometry and its application to changes in the Earth ' s surface. Reviews of Geophysics, 36(4), 441-500.
19. McCalpin, J. P., & Nishenko, S. P. (1996). Holocene paleoseismicity, temporal clustering, and probabilities of future large (M> 7) earthquakes on the Wasatch fault zone, Utah. Journal of Geophysical Research: Solid Earth, 101(B3), 6233-6253.
20. McCalpin, J.P. (2009) Paleoseismology. 2nd Edition, Academic Press, Amsterdam- London, 615 p. (International Series, 95).
21. Meltzner, A.J. (2010) Earthquake recurrence, clustering, and persistent 292 JOUR.GEOL.SOC.INDIA, VOL.95, March 2020 segmentation near the southern end of the 2004

Sunda megathrust rupture, Ph.D. thesis, Calif. Inst. of Technol., Pasadena. http://resolver.caltech.edu/ Caltechthesis: 06012010 082222484.
22. Mishra, S., & Prajapati, S. (2019). Crustal structure of Andaman Islands using joint inversion of receiver functions and surface wave dispersion measurements. Annals of Geophysics, 62(6), GT675-GT675.
23. Moores, E. M., Robinson, P. T., Malpas, J., & Xenophonotos, C. (1984). Model for the origin of the Troodos massif, Cyprus, and other mideast ophiolites. Geology, 12(8), 500-503.
24. Naik, G., Srivastayva, A., & Mishra, V. (1997). KDM Institute of Petroleum Exploration ONGC, Dehradun 248195, India. In Contemporary Lithospheric Motion Seismic Geology: Proceedings of the 30th International Geological Congress, Beijing, China, 4-14 August 1996 (Vol. 5, pp. 143-161). VSP.
25. Nakata, T., 1972, Geomorphic history and crustal movements of the foothills of the Himalayas. Report of Tohoku University Japan, 7th series (Geography), 22, pp. 39– 177.
26. Nakata, T., 1989, Active faults of the Himalaya of India and Nepal. Geological Society of America. Special Paper, 232, pp. 243–264
27. Ortiz, M., & Bilham, R. (2003). Source area and rupture parameters of the 31 December 1881 Mw. Journal of geophysical research, 108(B4), ESE11-1.
28. Pal, T. (2020). Structural imprints of Andaman accretionary prism and its tectonic relation with Ophiolite Belt of Indo-Burma ranges. Structural geometry of mobile belts of the Indian subcontinent, 111-130.
29. Pal, T., Gupta, T. D., Chakraborty, P. P., & Gupta, S. C. D. (2005). Pyroclastic deposits of mio-pliocene age in the Arakan Yoma-Andaman-Java subduction complex, Andaman Islands, Bay of Bengal, India. Geochemical Journal, 39(1), 69-82.
30. Philip, G. and Sah, M.P., 1999, Geomorphic signatures for active tectonics in the Trans-Yamuna segment of the western Doon valley, NW Himalaya. International Journal of Applied Earth Observation and Geoinformation, 1, pp. 54–63.
31. Philip, G. and Virdi, N.S., 2006, Co-existing compressional and extensional regimes along the Himalayan front vis-a` -vis active faults near Singhauli, Haryana, India. Current Science, 90, pp. 1267–1271.
32. Philip, G., 1996, Landsat Thematic Mapper data analysis for Quaternary tectonics in parts of Doon valley, NW Himalaya, India. International Journal of Remote Sensing, 17, pp. 143–153.
33. Philip, G.,2007, Remote sensing data analysis for mapping active faults in the northwestern part of Kangra Valley, NW Himalaya, India, International Journal of Remote Sensing, Vol. 28, No. 21, 4745–4761.
34. Rajendran, C. P., & Rajendran, K. (2020). On the trail of the great 2004 Andaman- Sumatra earthquake: seismotectonics and regional tsunami history from the Andaman- Nicobar segment. The Andaman Islands and Adjoining Offshore: Geology, Tectonics and Palaeoclimate, 205-222.
35. . San'kov V., Deverchere, J., Gaudemer, Y., Houdry, F. and Filippov, A., 2000, Geometry and rate of faulting in the North Baikal Rift, Siberia. Tectonics, 19, pp. 707– 722.
36. Valdiya, K.S., 1986, Neotectonic activities in the Himalayan belt. In Proceedings of the International Symposium on Neotectonics in South Asia (Dehradun: Survey of India), pp. 241–251.
37. Valdiya, K.S., 1993, Uplift and geomorphic rejuvenation of the Himalaya in the Quaternary period. Current Science, 64, pp. 873–885.
38. V. Teichrieb and J. Kelner, "Enhancement of radar based DEMs using 3D techniques," in Proceedings of the IEEE International Geoscience and Remote Sensing Symposium IGARSS '07), pp. 4902–4905, Barcelona, Spain, June 2007.

ISSN: 2278-4632
Vol-13, Issue-11, No.05, November: 2023

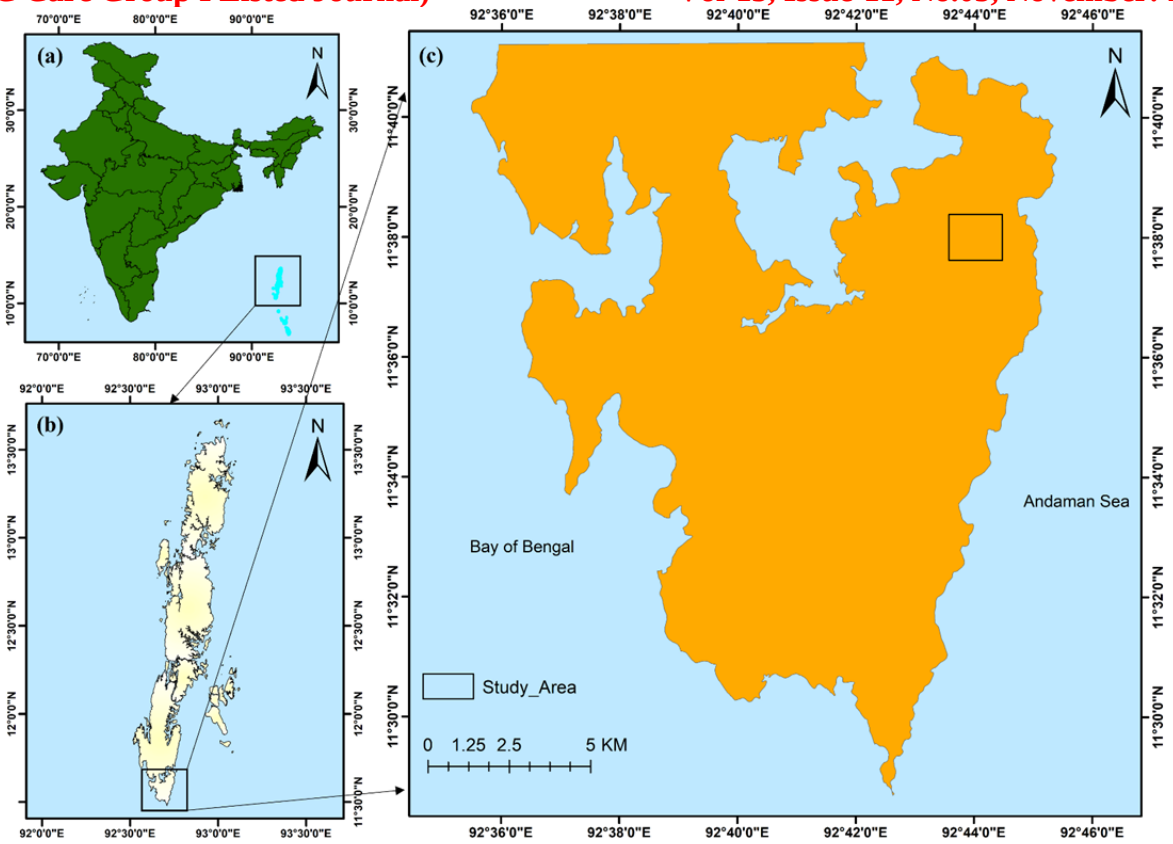

Figure.1: (a) India (b) Andaman Islands (c) Location of the study area

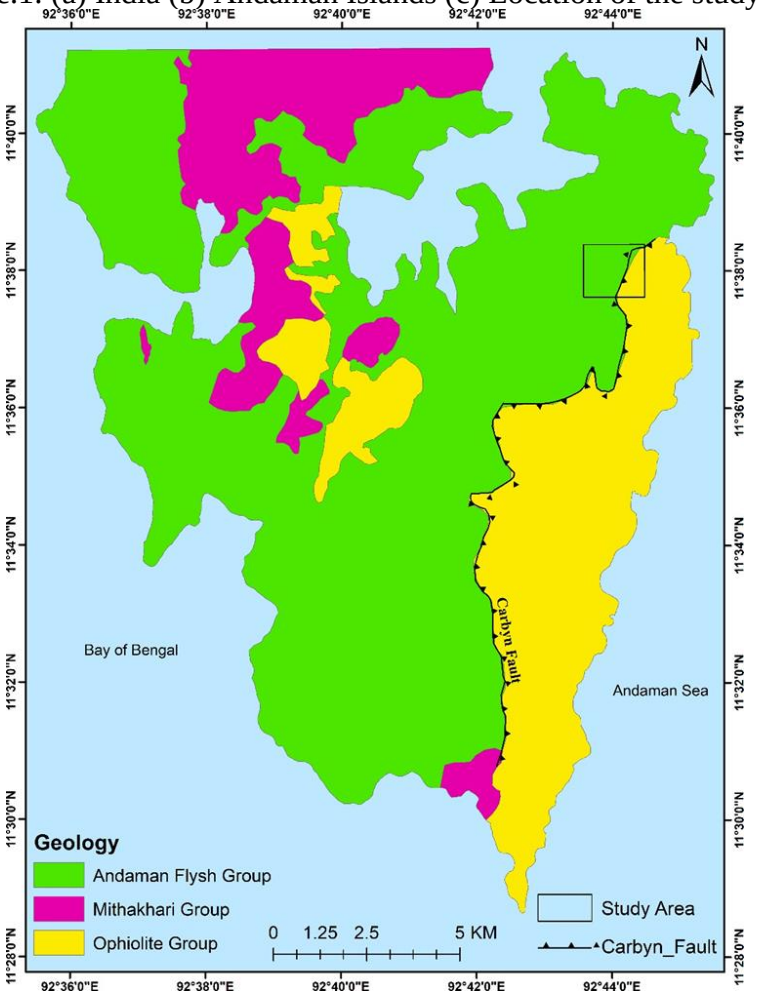

Figure.2: Geology map of the Study Area (modified after Bhat et al, 2020)

ISSN: 2278-4632
Vol-13, Issue-11, No.05, November: 2023

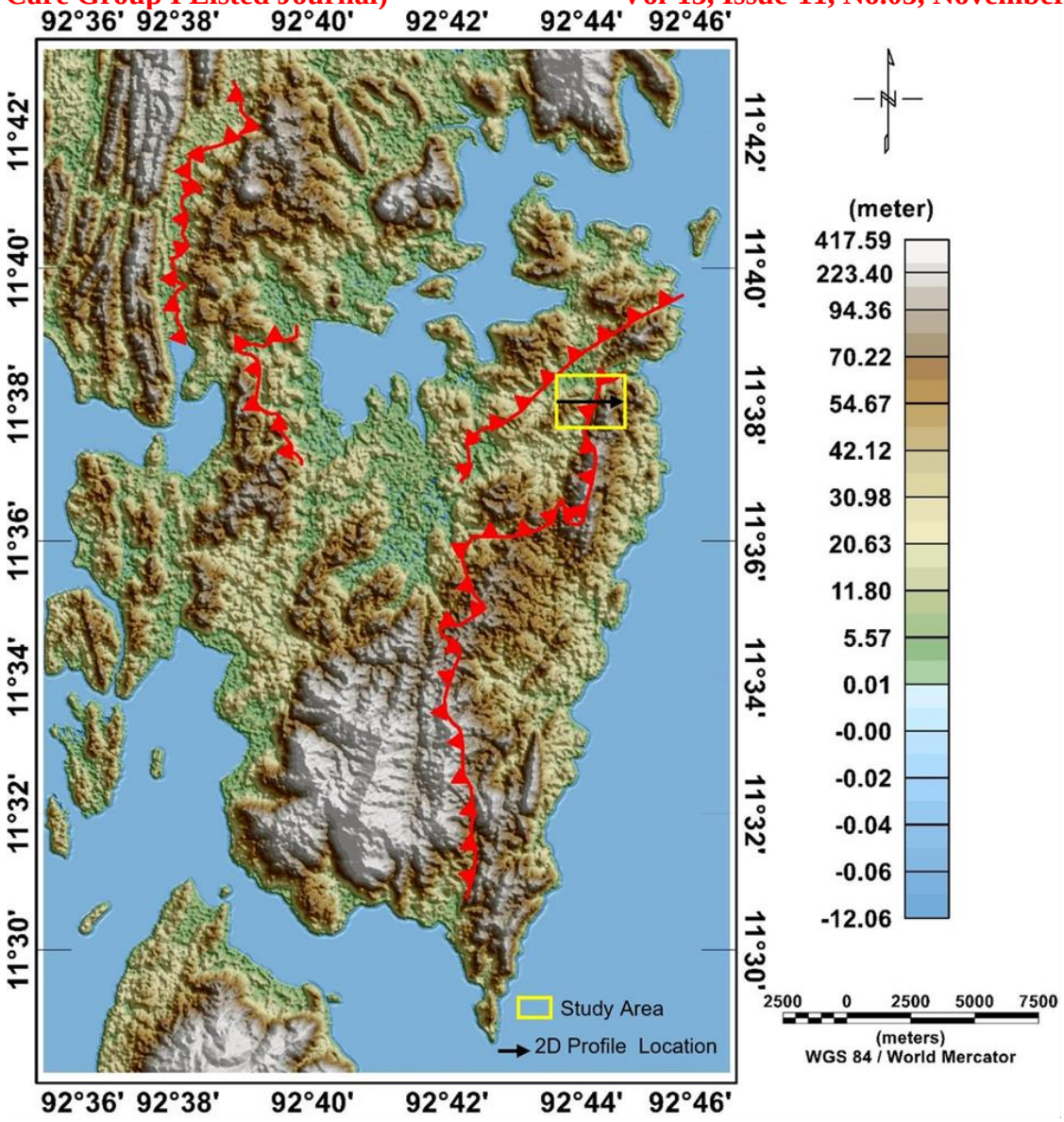

Figure.3: Digital Elevation Model with Fault line

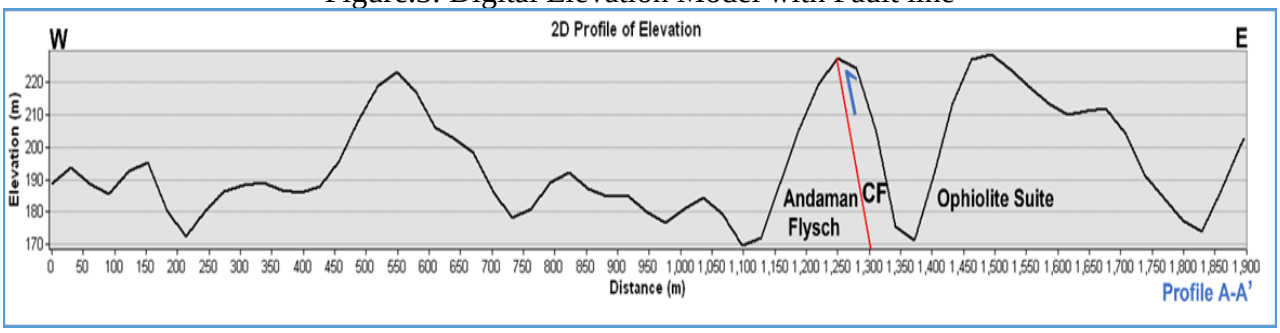

Figure.3a: 2D Elevation Profile

ISSN: 2278-4632
Vol-13, Issue-11, No.05, November: 2023

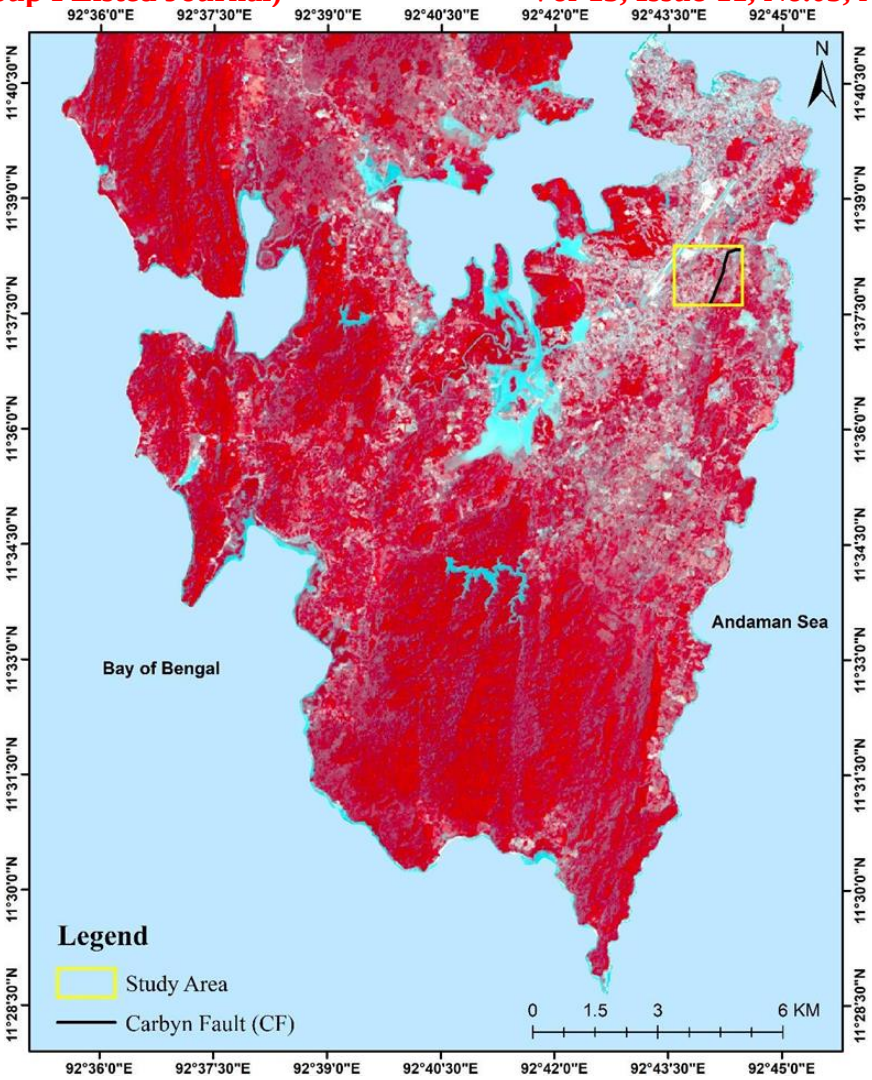

Figure.4: Pan Sharpened Landsat 8 OLI_TIRS (Band 2,3,4,5 & 8)

Table1: Datasets used in the current study

S. No.	Data	Description	Source	Date Acquired
1	Survey of India Toposheet	87A10	https://onlinemaps.surveyofindia.gov.in/	-
2	SRTM DEM (30m)	-	https://earthexplorer.usgs.gov/	-
3	Landsat 8 OLI_TIRS Panchromatic (15 m)	LC08_L1TP_134052_20220227_20220309_02_T1_B2.TIF LC08_L1TP_134052_20220227_20220309_02_T1_B3.TIF LC08_L1TP_134052_20220227_20220309_02_T1_B4.TIF LC08_L1TP_134052_20220227_20220309_02_T1_B5.TIF LC08_L1TP_134052_20220227_20220309_02_T1_B8.TIF	https://earthexplorer.usgs.gov/	27-02-2022
4	Google Earth Pro	-	-	-